Desalination and Water Treatment
www.deswater.com

doi: 10.5004/dwt.2021.26673

211 (2021) 349–358
January

High elimination of dye from synthetic aqueous solution by chemical treated sewage sludge

Meriem Zamouche[a,*], Ouarda Moumeni[b], Ismahan Mehcene[a], Manel Temmine[a]

[a]*Laboratoire de l'Ingénierie des Procédés de l'Environnement (LIPE), Département de Génie de l'Environnement, Faculté de Génie des Procédés, Université de Salah BOUBNIDER Constantine 3, Constantine, 25000, Algeria, Tel. +213 555 83 87 45; emails: meriem.zamouche@univ-constantine3.dz/zamouche_meriem@yahoo.fr (M. Zamouche), mehcene.ismahan@gmail.com (I. Mehcene), maneltemmine@gmail.com (M. Temmine)*

[b]*Laboratory of Process Engineering, Department of Process Engineering, Faculty of science and technology, Mohammed Cherif Messaadia University, Road of Annaba, P.O. Box: 1553, 41000 Souk-Ahras, Algeria, email: w.moumni@univ-soukahras.dz*

Received 18 March 2020; Accepted 3 October 2020

ABSTRACT

The adsorption potential of sewage sludge treated with sulfuric ($SS_{AS0.1}$), nitric ($SS_{AN0.1}$) and phosphoric ($SS_{AP0.1}$) acid for the cationic dye, Malachite Green (MG), was investigated. On the basis of the amount of dye adsorbed (9.52 mg/g), the treatment of sewage sludge with sulfuric acid was found to be the most suitable in comparison to the other two acids. The adsorption tests were carried out depending on the adsorbent dose (0.25–4 g), pH of the solution (3–11), temperature (288–318 K), and contact time. The amount of MG adsorbed by $SS_{AS0.1}$ was minimal at a very acidic pH (pH ≤ 3); the optimal pH found was 5. The adsorption of the dye decreases with increasing temperature, while it increases with rising initial dye concentration. Experimental data were examined by non-linear regression of Langmuir and Freundlich isothermal models. Analysis of the results obtained using the three error functions applied and the coefficient of determination revealed that the Langmuir isotherm describes well the adsorption of MG by $SS_{AS0.1}$ with a maximum monolayer capacity (q_{max}) of 95.98 mg/g. The adsorption mechanism of MG by $SS_{AS0.1}$ can be governed by the two steps of diffusion within the film and intraparticle diffusion, the adsorption process is of pseudo-second-order.

Keywords: Adsorption; Malachite Green; Chemically treated sewage sludge; Isotherm; Kinetics

1. Introduction

Dyes are widely used in printing, cosmetics, papers, and woods, they are also coloring food and pharmaceutical products, but especially in the textile industries for their chemical stability and the easy of their syntheses and their color varieties [1]. The use of synthetic dyes in various industrial applications can cause pollution of the environment, especially if these effluents are discharged into the receiving environment without prior treatment. Unfortunately, these contaminants will be found in lakes, rivers, and groundwater [2].

Dyes are unsaturated and/or aromatic organic compounds, which seriously harm the environment. Even at low concentrations, they influence the aesthetic value and reduce the penetration of light in aquatic life, which hinders the photosynthesis of aquatic plants. Consequently, aquatic life will be altered in its entirety. In addition, bioaccumulation of dyes poses a potential hazard to humans through transport through the food chain [1,3].

Triphenylmethane (triarylmethane) dyes are one of the groups of dyes that are most commonly used in the textile. This groups are recognized by their very recalcitrant nature which makes them more resistant to microbial degradation. This class contains compounds that generally have a

* Corresponding author.

Presented at the International Conference on Sustainable Water Treatment Technologies and Environment (SUST-WATER 2019), 14–16 October 2019, Tipasa, Algeria

net positive charge, a typical example is the malachite green dye (MG) [4].

Malachite green MG is widely used in aquaculture as a parasiticide, for the control of fungal infections, protozoan infections, and some other diseases caused by helminths on a wide variety of fish and other aquatic organisms. It is also used in food as coloring agent, a medical disinfectant and anthelmintic product as well as a dye in textile and other industries [5,6].

Various detrimental effects associated with malachite green have been reported in the study of Rangabhashiyam et al. [7], it can cause damage to the liver, intestines, kidneys, gills, gonads, and pituitary gonadotrophic cells. Is also cytotoxic, carcinogenic, and may cause irritation of the respiratory and gastrointestinal tract and redness of the skin, and permanent eye damage.

Various dye loaded effluent treatment techniques have been used out, such as coagulation–flocculation, photosynthesis oxidation, membrane techniques (ultrafiltration or reverse osmode), ion exchange, and biological processes [7].

Adsorption is also one of the most effective techniques for the treatment of colored effluents. This technique is easy to use, simple of design, and does not require a large investment, especially if the adsorbent used is not activated carbon. In this context, the use of natural waste or by-products for their recovery as adsorbent material seems to be a very interesting alternative. Different natural or byproducts materials have been successfully tested as adsorbent by researchers, for the removal of Malachite green from aqueous solution, that is, Brewers' spent grain [8], *Artocarpus odoratissimus* leaves [9]. *Luffa ayegyptica* peel waste [10], lemon peel [11], walnut shells [12], *Carica papaya* wood [7], natural sawdust mix composed of pine, oak, hornbeam, and fir biomasses [13], beech sawdust [14], and sugarcane bagasse [15].

In this work, our target is to study the adsorption of cationic dye, Malachite green, on sewage sludge, a municipal wastewater treatment byproduct, which can be valorized as an adsorbent.

In order to carry out this study, it was essential to examine a variety of parameters, such as: the effect of chemical treatment of sewage sludge by different acids, the effect of experimental operating parameters on the amount of dye adsorbed, and the modeled of experimental data by Langmuir and Freundlich isotherms equation, in order to get more information about adsorption type and mechanism.

2. Materials and methods

2.1. Adsorbent

The adsorbent employed in this work is sewage sludge from Ibn Zied municipal wastewater treatment plant of in Constantine, Algeria. The chemical treatment of the sewage sludge was carried out by mixing a fixed amount of sludge with a fixed volume of an acid solution at a concentration of 0.1 M.

The impregnation ratio was 25 (volume of acid solution/mass of adsorbent) for 24 h. Subsequently, the suspension was centrifuged at 3,000 rpm for 5 min to remove the activating agent. The recovered sludge has been washed several times with distilled water until pH and the conductivity of washing water were stable. Finally, the obtained sludge was dried at 378 K for 3 d and ground to a particle size of ≤315 μm. Three acids have been used for chemical treatment of sludge: nitric acid, phosphoric acid, and sulfuric acid.

2.2. Adsorbate

The dye used in this study, Malachite Green(MG) ($C_{23}H_{25}ClN_2$), is a cationic dye of the triarylmethane family which is a dark green-crystalline powder. The molecular weight of Malachite Green is 364.911 g/mol [13]. Malachite Green was supplied by Sigma-Aldrich (France), its molecular structure is shown in Fig. 1. The wavelength that corresponds to the maximum of absorbance, λ_{max}, was 616.5 nm.

2.3. Batch reactor adsorption test

The adsorption of MG by $SS_{AS0.1}$ was carried out in batch mode, at a T = 298 ± 1 K, in a 250 mL beaker. Thus, a mass of 0.5 g of sludge was mixed with 100 mL of an aqueous-dye solution with a concentration of 50 mg/L. This suspension was then agitated at a speed of 3,000 rpm with heating and agitating (Heidolph MR Hei-Standard) until equilibrium. Samples of 0.5 mL are sampled regularly over time until the adsorption equilibrium is achieved, then the suspension is centrifuged (centrifuge-Sigma 1–6P) at 3,000 rpm for 5 min. Subsequently, the supernatant is recovered and measured by spectrophotometer (Shimadzu mini 1240, France) in order to determinate the residual concentration of dye in solution. The adsorbed amount is calculated from the residual concentration in solution according to the following equation:

$$q_t = \frac{\left(C_0 - C_t\right)V}{m} \tag{1}$$

where C_0 is the initial dye concentration (mg/L), C_t is the concentration of the dye at time t (mg/L), V is the volume of the solution (L), m is the mass of the adsorbent (g), and q_t is the amount adsorbed at time t.

The dye removal percentage of adsorption is calculated as given below:

$$\text{Removal percentage } \% = \frac{\left(C_0 - C_e\right)100}{C_e} \tag{2}$$

where C_e (mg/L) is the equilibrium concentration in solution.

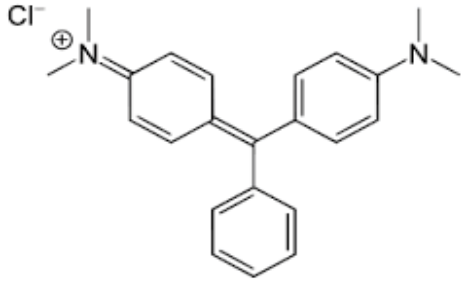

Fig. 1. Molecular structure of MG.

3. Results and discussion

3.1. Characterization of adsorbent

The point of zero charge (pH_{pzc}) was measured according to the method given by Leon y Leon and Radovic [16] and Moreno-Castilla et al. [17]. The measured zero point charge of activated sewage sludge used in this work ($SS_{AS0.1}$) is equal to 5.2.

The contents of acidic and basic functional groups of activated sewage sludge were determined by Boehm titration [18–20]. Table 1 shows the total functional groups of $SS_{AS0.1}$. As reported in Table 1, chemically activated sewage sludge is rich in acidic functional groups such as strong carboxylic acid and hydroxyl and phenolic groups. The increase in acidic functional groups is probably due to the chemical treatment of the sludge by sulfuric acid.

3.2. Effect of chemical acid treatment on sewage sludge

The effect of chemical sewage sludge treatment with the three different acids, namely nitric, sulfuric, and phosphoric acid, has been tested on the adsorption of Malachite Green. The results presented in Fig. 2 show that chemical treatment of sewage sludge with sulfuric acid produces the highest adsorbed amount of dye compared with the two other acids, followed by nitric acid and phosphoric acid, respectively (9.52, 8.17, and 8.1 mg/g).

Table 1
Surface functions of chemically treated sewage sludge ($SS_{AS0.1}$)

Concentration according to surface	m_{eq}/g
Strong carboxylic acid (G I)	0.15
Lactone and weak carboxylic acid (G II)	0
Hydroxyl and phenol (G III)	0.23
Total of acidic surface functions	0.38
Total of basic surface functions	0.04

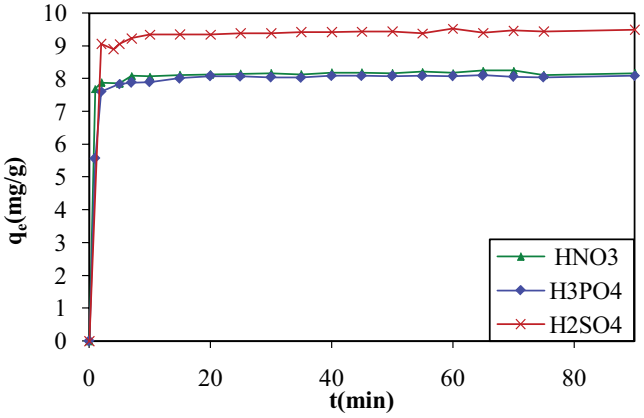

Fig. 2. Effect of chemical acid treatment on the sewage sludge tested on the MG adsorption. (C_0 = 50 mg/L, W = 300 rpm, m/v = 0.005 g/L, and T = 298 K).

This result is an extension of that obtained in 2016 [21], when studying the adsorption of Rhodamine by sewage sludge chemically treated with sulfuric acid. The same result was also obtained in the study given by Otero et al. [22], in which sewage sludge was activated by sulfuric acid and tested for the adsorption of phenol (P), crystal violet (CV), and indigo carmine (IC). However, sludge chemically treated with sulfuric acid was chosen to carry out the Malachite Green adsorption study for the remainder of this work.

3.3. Effect of operating parameters

3.3.1. Effect of adsorbent mass

The study of adsorbent mass effect (Fig. 3) shows that the percent dye removal increases from 93.45% to 96.12% when mass increases from 0.25 to 4 g, respectively. This can be attributed to the increase in the available surface area and the increase in active sites on the surface of the sewage sludge. As can be seen in Fig. 3, the adsorbent mass giving a maximum dye percent removal is 0.5 g. Although the percent removal obtained with a mass of 4 g is slightly higher than that achieved with the 0.5 g mass, this difference remains not important, so that 0.5 g mass is considered to be optimal.

3.3.2. Effect of temperature

The effect of solution temperature on the dye removal by $SS_{AS0.1}$ is presented in Fig. 4. The raising of solution temperature from 288 to 318 K results in a slight decrease in the amount of dye adsorbed by $SS_{AS0.1}$ (from 9.56 to 9.43 mg/g). This can be explained by the exo-thermicity of the adsorption process and the weakening of the bonds between the dye and the active adsorbent sites at higher temperatures [23–27].

The diminution of the adsorbed amount of dye with the raising of temperature is may be also attributed to the increasing of dye solubility as the solution temperature increasing which resulting in stronger interaction forces between MG and solute more than those between MG and

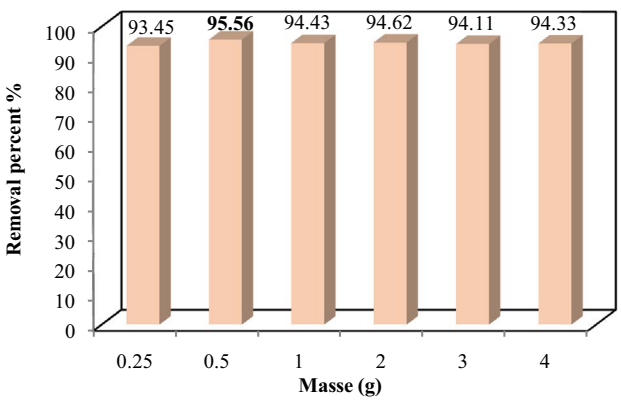

Fig. 3. Effect of adsorbent mass on the adsorption of MG. (C_0 = 50 mg/L, W = 300 rpm, and T = 298 K).

chemically activated sewage sludge. High temperature might also lead to the breaking of existing intermolecular hydrogen bonding between MG and $SS_{AS0.1}$, which can contributed to escape of MG ions from adsorbent phase to the bulk phase [27,28].

In addition, there is no significant effect of temperature on the adsorption capacity at equilibrium, the same result was observed during the adsorption of MG by the potato peel [29]. The highest amount of dye adsorbed by the chemically activated sewage sludge (9.56 mg/g) was recorded at a temperature of 298 K; this temperature was considered optimal for the remainder of this work.

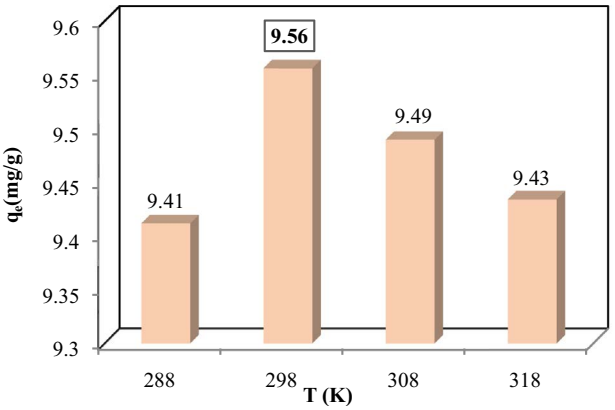

Fig. 4. Effect of solution temperature on the removal of MG by $SS_{AS0.1}$. (C_0 = 50 mg/L, W = 300 rpm, and m = 0.5 g).

3.3.3. Effect of concentration and contact time

The effect of the initial dye concentration on the adsorption of Malachite Green by chemically treated sewage sludge was investigated between 25 and 300 mg/L. The equilibrium amount adsorbed as function of the initial concentration of dye is tabulated in Table 2. The results achieved show that the increasing in the initial concentration of the dye remarkably enhanced the equilibrium amount of Malachite Green adsorbed. This increase is due to the increase in mortice force as the initial dye concentration increases. The amount of dye adsorbed at equilibrium increased from 4.59 to 54.64 mg/g when the initial concentration of dye increased from 25 to 300 mg/L. The equilibrium time was very faster: it was estimated by 2 min for a concentration of 25 mg/L and between 10 and 20 min for the other concentrations examined. A rapid equilibrium time is a desirable criterion for the practical implementation of the depollution by the adsorption process.

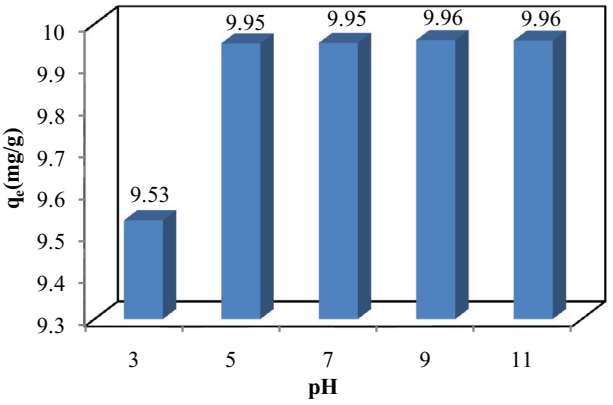

Fig. 5. Effect of pH solution on the dye adsorption. (C_0 = 50 mg/L, W = 300 rpm, $m_{optimal}$ = 0.5 g, and $T_{optimal}$ = 298 K).

3.3.4. Effect of pH

For the examination of this effect, the pH range considered was 3–11, and below or above this range a decrease in the color intensity of the MG was observed. This was reported in the study given by Adeyi et al. [27] and Dahri et al. [30], where they observed that at a very acidic pH (pH < 3), there was a clear reduction in color intensity without any change in the wavelength of maximum absorption (λ_{max}). The reduction in color intensity at pH < 3 is due to the formation of MGH^{2+} species as reported by Dahri et al. [30].

As is shown in Fig. 5, at a strongly acidic pH (pH = 3), a low adsorption capacity (9.53 mg/g) was obtained. At this pH, the adsorbent is positively charged (pH < pH_{pzc} = 5.2) while the MG is cationic, which induces a repulsion between the adsorbent and the dye. On the other hand, the concentration of H^+ protons in the solution was high, resulting in competition between the protons and the dye to occupy the free adsorption sites on the adsorbent [31]. In the pH range [5–11], the adsorption capacity increased to 9.95 mg/g (≈99%), corresponding to an almost complete removal rate, and remained unchanged. In this pH range, the surface of the sludge is negatively charged (pH > pH_{pzc} = 5.2) and the dye is still cationic which induces an attraction between the dye and the sludge surface, therefore the amount adsorbed has increased. In addition, the presence of acidic surface functions on the surface of chemically activated sewage sludge (Table 1) contributes advantageously to the removal of the cationic dye. The optimum pH chosen is 5, corresponding to the maximum dye adsorption. A similar result was given by Adeyi et al. [27], in the case of the MG adsorption by hydrophilic thiourea-modified [27].

Table 2
Evolution of equilibrium time and equilibrium adsorbed amount for different initial dye concentration

Temperature	Concentration (C_0 mg/L)	25	50	100	150	200	250	300
298 K	t_e (min)	2	10	10	15	20	10	15
	q_e (mg/L)	4.59	9.55	19.41	29.05	38.11	46.23	54.64

3.4. Kinetics and mechanism adsorption

Both pseudo-first-order and pseudo-second-order kinetic models were applied to analyze the experimental data of MG adsorption by $SS_{AS0.1}$. The pseudo-first-order kinetic equation, also known as the Lagergren equation, and the pseudo-second-order kinetic equation proposed by Blanchard [31,32] are shown in Table 3.

The plots of $\ln(q_e - q_t)$ vs. time (t) for the pseudo-first-order model and the plots of t/q_t as a function of time (t) for the pseudo-second-order model are shown in Fig. 6. The kinetic parameters calculated by Blanchard and Lagergren are summarized in Table 3.

The plots of t/q_t vs. (t) for all concentrations studied (Fig. 6) show very good linearization. This is verified by the high values of the correlation coefficients obtained for all the concentrations studied (0.999). The correlation coefficient is not the only parameter indicating the applicability of a kinetic model, it is important to verify the agreement between the values of the experimental capacities (q_{exp}) and those calculated (q_{calc}). As shown in Table 3, it is clear that for the pseudo-first-order model, there is a large discrepancy between q_{exp} and q_{calc}, as well as low values of correlation coefficients, which means that this model is not applicable to describe the kinetic data of MG adsorption by $SS_{AS0.1}$.

While, for the pseudo-second-order model the calculated values of adsorption capacities (q_{calc}) coincide very well with the experimental data (q_{exp}). These indicate that the adsorption of MG by the sludge is pseudo-second-order.

Intraparticle diffusion model, based on the theory proposed by Weber and Morris [33] was tested to identify the diffusion mechanism. The evolution of the amount adsorbed as function of the square root of time at different

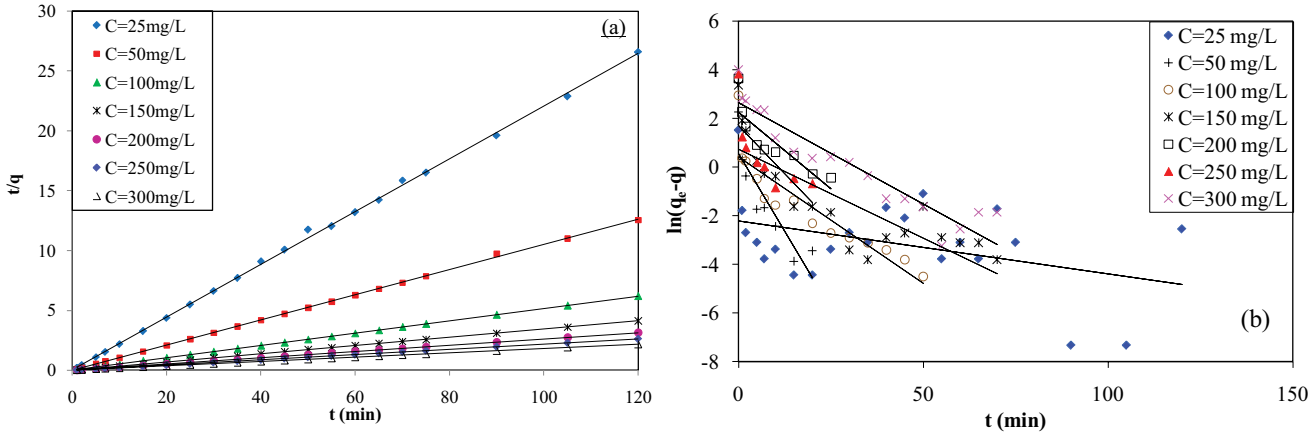

Fig. 6. Kinetic investigations on $SS_{AS0.1}$ pseudo-first-order (a) and pseudo-second-order models (b).

Table 3
Kinetic parameters of MG adsorption on $SS_{AS0.1}$

	Pseudo-first-order (Lagergren)				Pseudo-second-order (Blanchard)			
	$\frac{dq_t}{dt} = K_1(q_e - q_t)$				$\frac{dq_t}{dt} = K_2(q_e - q_t)^2$			
	Linearized form: $\ln(q_e - q_t) = \ln q_e - K_1 t$				Linearized form: $\frac{t}{q_t} = \frac{1}{K_2 q_e^2} + \frac{1}{q_e} t$ With initial adsorption rate h: $h = q_e^2 K_2$			
Initial MG concentration (mg/L)	q_{exp} (mg/g)	q_{calc} (mg/g)	K_1 (1/min)	R^2	q_{calc} (mg/g)	K_2 (g/mg min)	h (mg/g min)	R^2
25	4.59	0.11	0.022	0.167	4.54	1.015	20.92	0.999
50	9.56	1.70	0.254	0.789	9.51	1.165	105.26	0.999
100	19.41	1.52	0.104	0.814	19.42	0.323	121.95	0.999
150	29.06	2.07	0.073	0.678	29.15	0.147	125.00	0.999
200	38.11	9.46	0.125	0.745	38.46	0.059	87.72	0.999
250	46.23	5.42	0.158	0.543	46.30	0.179	384.62	0.999
300	54.64	13.99	0.083	0.889	55.56	0.021	64.10	0.999

initial dye concentrations is presented in Fig. 7. The parameters of the Weber and Morris model are summarized in Table 4.

If intraparticle diffusion is involved in the adsorption process, then the plot of uptake, q_t, as function of the square root of time ($t^{1/2}$) should be linear and if these lines pass through the origin, then intraparticle diffusion process that controls the rate of diffusion. When the plots do not pass through the origin, the intraparticle diffusion is not the only rate-limiting step, but other kinetic models may also control the adsorption rate, or all may operate simultaneously [34]. As shown in Fig. 7, the resulting plots do not pass through the origin and they are multilinear containing three segments, which means that the intraparticle diffusion is involved in the adsorption process but other kinetic models may also be involved in controlling the adsorption kinetics. Based on the values of the correlation coefficients obtained for all concentrations studied (Table 4), the linearity of the segments was approved. Thus, the first linear segments represent diffusion in the film; the second linear segments represent diffusion in the pores. The last segment is the final step before equilibrium where intraparticle diffusion begins to slow due to the low concentration of solute in solution [35].

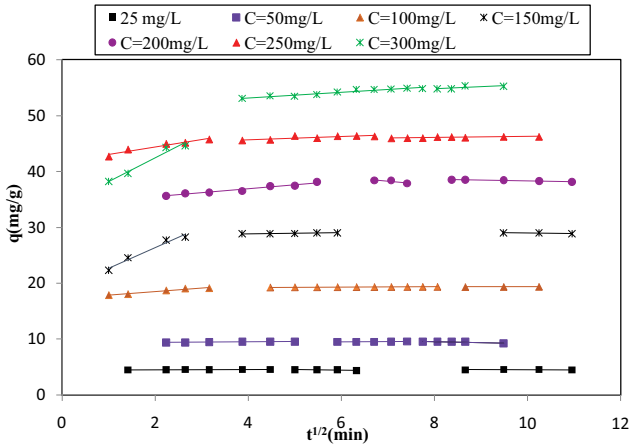

Fig. 7. Evolution of dye adsorbed amount as a function of the square root of time for various initial dye concentration at T = 298 K.

Overall, the increase in the initial dye concentration results in an increase in the y-intercept value calculated for all concentrations studied. This indicates that intra-particle scattering is less and less involved in the adsorption process. The y-intercept (c-value) of the three linear portions is a measure of the thickness of the boundary layer, the higher the c-value, the greater the contribution of external diffusion in limiting the rate of adsorption [32].

Boyd model was considered to identify the implication of film diffusion and intra-particle diffusion, in the adsorption mechanism, this model is given by the following expression [36,37]:

$$B_t = -0.4978 - \ln\left(1 - F\right) \tag{3}$$

where F is the fraction of the adsorbed solute at time t and it is given as follows:

$$F = \frac{q_t}{q_e} \tag{4}$$

If the plot of B_t vs. time is a straight line and passes through the origin, this implies that intraparticle diffusion is the limiting step in the adsorption rate. Otherwise, it is governed by the film diffusion (external diffusion) mechanism [36,37].

As shown in Fig. 8, the plot of B_t as a function of time for all the initial dye concentrations studied, does not pass through the origin and they practically non-linear; indicating that film diffusion may also contribute to limiting the adsorption rate [37,38].

3.5. Isotherm adsorption

The experimental adsorption isotherms of MG from aqueous solutions onto $SS_{AS0.1}$ are presented in Fig. 9. Giles et al. [39] have been classified the adsorption isotherms into four groups, which are: *L*, *S*, *H*, and finally, *C*. By referring to this classification, the isotherm of MG presented an *L* curve shape (also named Langmuir). The *L* shape means flat adsorption of bifunctional molecules, that is to say, a decrease in free sites as the adsorption proceeds, this suggests a progressive saturation of the solid [40,41]. The *L* form of the adsorption isotherms also means that there

Table 4
Weber and Morris model parameters and correlation coefficients for different initial dye concentrations at T = 298 K

Webber and Morris	Equation	25	50	100	150	200	250	300
K_1 (mg/g min$^{1/2}$)	$q_t = K_i t^{1/2} + c$ [27] K_i (mg/g min$^{1/2}$), the intraparticle diffusion rate constant and c is the intercept	0.018	0.071	0.641	3.682	0.72	1,307	4,259
C_1		4.50	9.273	17.232	19.02	33.01	41.758	33,898
r_1^2		0.841	0.873	0.97	0.986	0.962	0.967	0.964
K_2 (mg/g min$^{1/2}$)		0.099	0.029	0.023	0.109	–0.73	0.28	0.645
C_2		5.07	9.71	19.12	28.435	43.37	44.548	50.218
r_2^2		0.616	0.645	0.980	0.863	0.712	0.667	0.898
K_3 (mg/g min$^{1/2}$)		0.028	–0.183	0.028	–0.973	–0.144	0.088	0.357
C_3		4,306	11.036	19.125	29.944	39.716	45.371	51.924
r_3^2		0.770	0.771	0.999	0.791	0.961	0.671	0.555

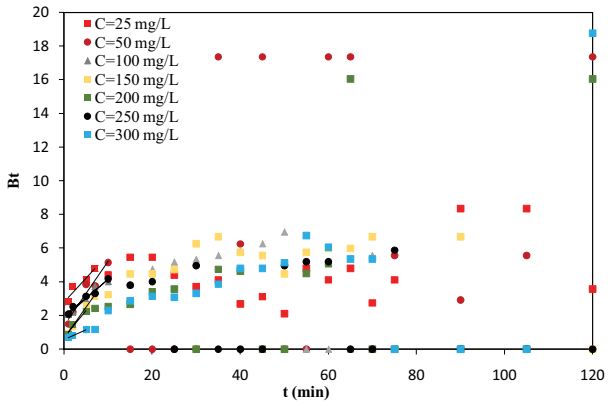

Fig. 8. Kinetic model of Boyd for various MG initial concentration at T = 298 K.

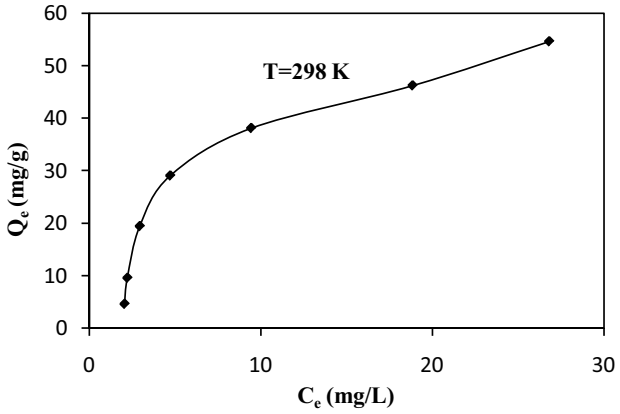

Fig. 9. Adsorption isotherms of MG by $SS_{AS0.1}$ at T = 298 K.

is not a strong competition between the solvent and the adsorbent to occupy the adsorption sites [40].

The Langmuir adsorption isotherm describes the surface as homogeneous, assuming that there is no lateral interaction between adjacent adsorbed molecules when a single molecule occupies a single surface site [42,43]. The nonlinear equation of Langmuir is given in Table 5, where Q_m (mg/g) is the maximum adsorption capacity of dye per unit mass of adsorbent to form a complete monolayer on the surface and K_L (L/mg) is the Langmuir energy constant.

Freundlich isotherm is known to describe the non-ideal and reversible adsorption, which was not restricted to the formation of monolayer. This empirical model is applied to multilayer adsorption over the heterogenous surface [42,44]. This isotherm gives an expression that defines the surface heterogeneity and the exponential distribution of active sites and their energies [45,46]. The non-linear equation of Freundlich is given in Table 5, where K_F is adsorption capacity (L/mg) and $1/n$ is adsorption intensity.

The Langmuir and Freundlich isothermal parameters were calculated by the non-linear regression method. This method is based on minimizing the error distribution (between the measured (experimental) data and the predicted (isothermal) data [46,47]. In this study, three different non-linear error functions were used (Table 5), the isothermal parameters were determined by minimizing the respective error function across the studied concentration range using the Solver application of Microsoft Excel [47,48].

The results obtained are surmised in Table 6. Fig. 10 shows the Langmuir and Freundlich adsorption isotherms of the $SS_{AS0.1}$ by nonlinear analysis. The coefficient of determination (R^2) (Table 5) was also used to determine the best-fitting isotherm to the experimental data.

Table 5
Error function equation and isotherm equation of Langmuir and Freundlich

Error function equation	Abbreviation	Equation
Sum squares errors	SSE	$\mathrm{SSE} = \sum\left(q_{e,\mathrm{cal}} - q_{e,\mathrm{exp}}\right)^2$
Nonlinear chi-square test	χ^2	$\chi^2 = \sum_i^n \frac{\left(q_{e,\mathrm{meas}} - q_{e,\mathrm{calc}}\right)^2}{q_{e,\mathrm{meas}}}$
Sum of the absolute errors	EABS	$\mathrm{SSE} = \sum_{i=1}^{n}\left\lvert q_{e,i\ \mathrm{exp}} - q_{e,i\ \mathrm{calc}}\right\rvert$
Coefficient of determination	R^2	$R^2 = \frac{\sum\left(q_{e,\mathrm{meas}} - \overline{q}_{e,\mathrm{calc}}\right)^2}{\sum\left(q_{e,\mathrm{meas}} - \overline{q}_{e,\mathrm{calc}}\right)^2 + \sum\left(q_{e,\mathrm{meas}} - q_{e,\mathrm{calc}}\right)^2}$
Isotherm model	**Non-linear equation**	
Langmuir [33]		$Q_e = \frac{K_L Q_m C_e}{1 + K_L C_e}$
Freundlich [33]		$Q_e = K_F C_e^{\frac{1}{n}}$

where $q_{e,\text{meas}}$ is the equilibrium capacity obtained from experimental data, $q_{e,\text{calc}}$ is that calculated from the isotherm model and $\bar{q}_{e,\text{calc}}$ is the average of $q_{e,\text{calc}}$.

The choice of the isothermal model that best predicts the experimental data is based on the comparison of the values of determinations coefficient, the error function, and the nonlinear regression plot [30].

According to the nonlinear regression plot by Langmuir and Freundlich isotherms (Fig. 10), it is quite clear that the Langmuir model gives a better fit of the experimental data than Freundlich.

Furthermore, the high values of determination coefficient reported in Table 6, confirm the good fit of the predicted values to the experimental data. The R^2 obtained with the nonlinear regression of Langmuir is higher than that given by Freundlich model (0.996 > 0.993).

Moreover, by comparing the values of the three error functions SSE, EABS, and χ^2, it is clear that the Langmuir model has the lowest error function value. Among the three error functions tested, χ^2 gives the smallest value (11.69). Based on these observations, Langmuir isotherm has been chosen as the isothermal model that fits adequately the adsorption experimental data of MG by $SS_{AS0.1}$.

The predicted maximum monolayer capacity (95.98 mg/g) was similar to the experimental one (Fig. 10). This value was comparable to some adsorbent materials as summarized in Table 7.

The value of the (1/*n*) is between 0 and 1, which indicates that the adsorption of MG by the $SS_{AS0.1}$ is favorable [42–44,49].

4. Conclusion

Sulfuric acid activated sewage sludge ($SS_{AS0.1}$), a by-product of wastewater treatment, can be effectively recovered as a low-cost adsorbent to remove the cationic dye, Malachite Green (MG), from the aqueous solution. The adsorption process was found to be pH-dependent, with maximum dye removal being achieved at an optimum pH of 5. The amount of MG adsorbed increased as the initial concentration of MG increased. The adsorption process was very rapid and exothermic. Both intra- and extra-granular transfer steps are involved in the adsorption mechanism and the adsorption kinetics of MG is pseudo-second-order. The adsorption of the dye by the slurry is well-described by the Langmuir model with a maximum saturation capacity of 95.98 mg/g.

Table 6
Isotherm parameters of Langmuir and Freundlich obtained by nonlinear regression with different error function and their R^2 value

Model	Parameters	SSE	EABS	χ^2	R^2
Langmuir	Q_m (mg/g)	74.92	72.27	95.98	
	K_L (L/mg)	0.10	0.12	0.054	0.96
Value of error functions		124.16	22.81	11.69	
Freundlich	K_F (mg/g (L/mg)$^{1/n}$)	9.54	10.88	5.87	
	n	1.84	2.03	1.40	0.93
Value of error functions		209.66	29.68	15.68	

Table 7
Comparison of q_{max} values of different adsorbents for MG adsorption

	Adsorbent	q_{max} (mg/g)	Reference
1	Chemical treated sewage sludge ($SS_{AS0.1}$)	95.98	This work
2	*Casuarina equisetifolia* cone (CEC)	58.14	[50]
3	Breadfruit skin (BS)	55.2	[51]
4	*Luffa aegyptica* peel (LAP)	166.67	[10]
5	Cheap nano-adsorbent derived from eggshells	3,333.33	[52]
6	*Artocarpus odoratissimus* (Tarap) leaves	254.9	[53]
7	Brewers' spent grain	2.55	[8]
8	Ginger waste	84.03	[54]
9	Neem sawdust (*Azadirachta indica*)	4.35	[55]
10	Oil palm trunk fibre (OPTF)	149.35	[56]
11	Clayey soil	78.57	[57]
12	Hen feathers	2.82 (mol g)	[58]
13	Rattan sawdust	62.71	[59]
14	Bitter gourd	240.0	[60]
15	Bentonite	178.6	[61]

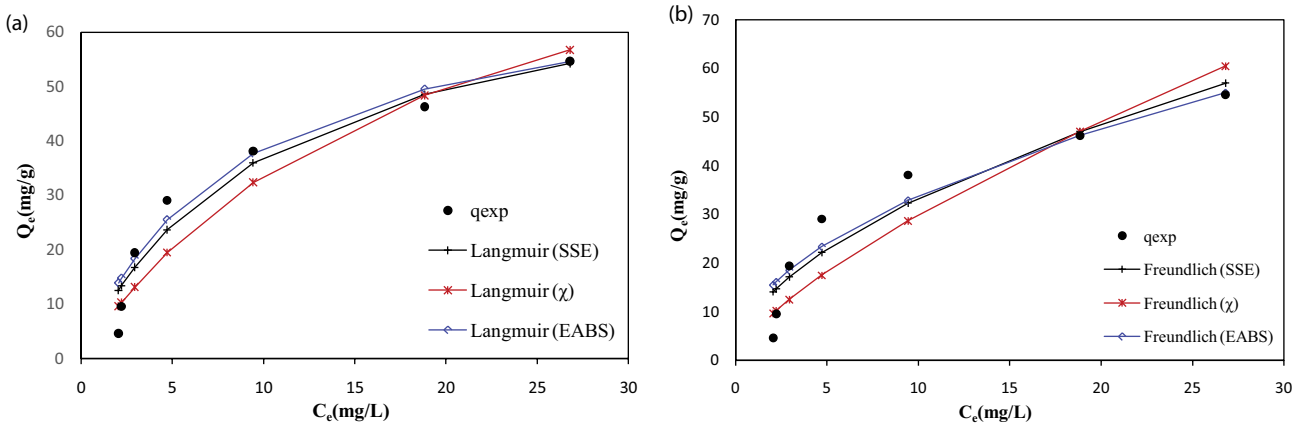

Fig. 10. Comparison between experimental and predicted isotherms (nonlinear regression of Langmuir and Freundlich) of MG adsorption onto $SS_{AS0.1}$ based on error function.

In the end, the chemical treated sewage sludge can be valorized and used as an efficient adsorbent, to eliminate the malachite green dye from the aqueous solution.

References

[1] H. Ben Mansour, O. Boughzala, D. Dridi, D. Barillier, L. Chekir-Ghedira, R. Mosrati, Textile dyes as sources of water contamination: screening for toxicity and treatment methods, J. Water. Sci., 24 (2011) 209–238.

[2] G.V. Brião, S.L. Jahn, E.L. Foletto, G.L. Dotto, Adsorption of crystal violet dye onto a mesoporous ZSM-5 zeolite synthetized using chitin as template, J. Colloid Interface Sci., 508 (2017) 313–322.

[3] T. Ngulube, J.R. Gumbo, V. Masindi, A. Maity, Calcined magnesite as an adsorbent for cationic and anionic dyes: characterization, adsorption parameters, isotherms and kinetics study, Heliyon, 4 (2018) 1–31, doi: 10.1016/j.heliyon.2018.e00838.

[4] Y.F. Tan, Removal of Triphenylmethane Dyes Using *Pseudomonas* Species, Bachelor of Science Biotechnology, University of Tunku Abdul Rahman, Malaysia, 2015

[5] S. Srivastava, R. Sinha, D. Roy, Toxicological effects of malachite green, Aquat. Toxicol., 66 (2004) 319–329.

[6] A.K. Srivastav, D. Roy, Acute toxicity of malachite green (triarylmethane dye) and pyceze (bronopol) on carbohydrate metabolism in the freshwater fish *Heteropneustes fossilis* (Bloch), Int. J. Fish. Aquat. Stud., 6 (2018) 27–30.

[7] S. Rangabhashiyam, S. Lata, P. Balasubramanian, Biosorption characteristics of methylene blue and malachite green from simulated wastewater onto *Carica papaya* wood biosorbent, Surf. Interfaces, 10 (2018) 197–215.

[8] H.A. Chanzu, J.M. Onyari, P.M. Shiundu, Brewers' spent grain in adsorption of aqueous Congo Red and malachite Green dyes: batch and continuous flow systems, J. Hazard. Mater., 380 (2019) 1–8, doi: 10.1016/j.jhazmat.2019.120897.

[9] N.A.H.M. Zaidi, L.B.L. Lim, A. Usman, Enhancing adsorption of malachite green dye using base-modified *Artocarpus odoratissimus* leaves as adsorbents, Environ. Technol. Innovation, 13 (2019) 211–223.

[10] F. Mashkoor, A. Nasar, Preparation, characterization and adsorption studies of the chemically modified *Luffa aegyptica* peel as a potential adsorbent for the removal of malachite green from aqueous solution, J. Mol. Liq., 274 (2019) 315–327.

[11] K. Vasanth Kumar, Optimum sorption isotherm by linear and non-linear methods for malachite green onto lemon peel, Dyes Pigm., 74 (2007) 595–597.

[12] S. Hajialigol, S. Masoum, Optimization of biosorption potential of nano biomass derived from walnut shell for the removal of Malachite Green from liquids solution: experimental design approaches, J. Mol. Liq., 286 (2019) 1–8, doi: 10.1016/j.molliq.2019.110904.

[13] F. Deniz, R.A. Kepekci, Bioremoval of Malachite green from water sample by forestry waste mixture as potential biosorbent, Microchem. J., 132 (2017) 172–178.

[14] A. Witek-Krowiak, Analysis of influence of process conditions on kinetics of malachite green biosorption onto beech sawdust, Chem. Eng. J., 171 (2011) 976–985.

[15] D.G. Vyavahare, G.R. Gurav, P.P. Jadhav, R.R. Patil, B.C. Aware, P.J. Jadhav, Response surface methodology optimization for sorption of Malachite Green dye on sugarcane bagasse biochar and evaluating the residual dye for phyto and cytogenotoxicity, Chemosphere, 194 (2018) 306–315.

[16] C.A. Leon y Leon, L.R. Radovic, Interfacial chemistry and electrochemistry of carbon surfaces, Chem. Phys. Carbon, 24 (1994) 213–310.

[17] C. Moreno-Castilla, M.V. López-Romón, F. Carrasco-Marín, Change in surface chemistry of activated carbons by wet oxidation, Carbon, 38 (2000) 1995–2001.

[18] H.P. Boehm, Surface oxides on carbon and their analysis: a critical assessment, Carbon, 40 (2002) 145–149.

[19] H.P. Boehm, Chemical identification of surface groups, Adv. Catal., 16 (1966) 179–274.

[20] C.A. Leon y Leon, J.M. Solar, V. Calemma, L.R. Radovic, Evidence for the protonation of basal plane sites on carbon, Carbon, 30 (1992) 797–811.

[21] I. Dincer, C. Ozgur Colpan, O. Kizilkan, M. Akif Ezan (Eds.), Progress in Clean Energy, Vol. 1, Analysis and Modeling, Springer International Publishing, Switzerland, 2015, pp. 623–630.

[22] M. Otero, F. Rozada, L.F. Calvo, A.I. García, A. Morán, Elimination of organic water pollutants using adsorbents obtained from sewage sludge, Dyes Pigm., 57 (2003) 55–65.

[23] Z. Aksu, A.B. Akın, Comparison of Remazol Black B biosorptive properties of live and treated activated sludge, Chem. Eng. J., 165 (2010) 184–193.

[24] I.A.W. Tan, A.L. Ahmad, B.H. Hameed, Adsorption of basic dye using activated carbon prepared from oil palm shell: batch and fixed bed studies, Desalination, 225 (2008) 13–28.

[25] S. Chowdhury, P.D. Saha, Biosorption of methylene blue from aqueous solutions by a waste biomaterial: hen feathers, Appl. Water Sci., 2 (2012) 209–219.

[26] T.K. Roy, N.K. Mondal, Biosorption of Congo Red from aqueous solution onto burned root of *Eichhornia crassipes* biomass, Appl. Water Sci., 7 (2017) 1841–1854.

[27] A.A. Adeyi, S.N.A.M. Jamil, L.C. Abdullah, T.S.Y. Choong, Adsorption of Malachite Green dye from liquid phase using hydrophilic thiourea-modified poly(acrylonitrile-*co*-acrylic acid): kinetic and isotherm studies, J. Chem., 4 (2019) 1–14.

[28] A.M. Aljeboree, A.N. Alshirifi, A.F. Alkaim, Kinetics and equilibrium study for the adsorption of textile dyes on coconut shell activated carbon, Arabian J. Chem., 10 (2017) S3381–S3393.

[29] E.K. Guechi, O. Hamdaoui, Sorption of malachite green from aqueous solution by potato peel: kinetics and equilibrium modeling using non-linear analysis method, Arabian J. Chem., 9 (2016) S416–S424.
[30] M.K. Dahri, M.R.R. Kooh, L.B.L. Lim, Water remediation using low cost adsorbent walnut shell for removal of malachite green: equilibrium, kinetics, thermodynamic and regeneration studies, J. Environ. Chem. Eng., 2 (2014) 1434–1444.
[31] I. Shah, R. Adnan, W.S. Wan Ngah, N. Mohamed, Iron impregnated activated carbon as an efficient adsorbent for the removal of methylene blue: regeneration and kinetics studies, PLoS One, 10 (2015) 1–23, doi: 10.1371/journal.pone.0122603.
[32] D. Suteu, T. Malutan, Industrial cellolignin wastes as adsorbent for removal of methylene blue dye from aqueous solutions, Bioressources, 8 (2013) 427–446.
[33] W.J. Weber, J.C. Morris, Advances in Water Pollution Research, Proceedings of International Conference on Water Pollution Symposium, Vol. 2, Pergamon, Oxford, 1962, pp. 231–266.
[34] N. Caner, I. Kiran, S. Ilhan, C.F. Iscen, Isotherm and kinetic studies of Burazol Blue ED dye biosorption by dried anaerobic sludge, J. Hazard. Mater., 165 (2009) 279–284.
[35] B.H. Hameed, M.I. El-Khaiary, Removal of basic dye from aqueous medium using a novel agricultural waste material: pumpkin seed hull, J. Hazard. Mater., 155 (2008) 601–609.
[36] H. Hafdi, M. Joudi, J. Mouldar, B. Hatimi, H. Nasrellah, M.A. El Mhammedi, M. Bakasse, Design of a new low cost natural phosphate doped by nickel oxide nanoparticles for capacitive adsorption of reactive red 141 azo dye, Environ. Res., 184 (2020) 1–14, doi: 10.1016/j.envres.2020.109322.
[37] S. Akbarnejad, A.A. Amooey, S. Ghasemi, High effective adsorption of acid fuchsin dye using magnetic biodegradable polymer-based nanocomposite from aqueous solutions, Microchem. J., 149 (2019) 1–12, doi: 10.1016/j.microc.2019.103966.
[38] S. Das, S. Mishra, Insight into the isotherm modelling, kinetic and thermodynamic exploration of iron adsorption from aqueous media by activated carbon developed from *Limonia acidissima* shell, Mater. Chem. Phys., 245 (2020) 1–20, doi: 10.1016/j.matchemphys.2020.122751.
[39] C.H. Giles, T.H. Mac Ewan, S.N. Nakhwa, D. Smith, A system of classification of solution adsorption isotherms, and its use diagnosis of adsorption mechanisms and in measurements of specific surface areas of solids, Studies in adsorption. Part XI, J. Chem. Soc., 10 (1960) 3973–3993.
[40] F. Edeline, The Physico-Chemical Purification, Theory and Technology of Water, 4th ed., Paris Lavoisier Tec & Doc impr, Cebedoc Sprl, Liège, 1998.
[41] G. Limousin, J.-P. Gaudet, L. Charlet, S. Szenknect, V. Barthes, M. Krimissa, Sorption isotherms: a review on physical bases, modeling and measurement, Appl. Geochem., 22 (2007) 249–275.
[42] R. Ramadoss, D. Subramaniam, Adsorption of chromium using blue green algae-modeling and application of various isotherms, Int. J. Chem. Technol., 10 (2018) 1–22.
[43] R. Saadi, Z. Saadi, R. Fazaeli, N. Elmi Fard, Monolayer and multilayer adsorption isotherm models for sorption from aqueous media, Korean J. Chem. Eng., 32 (2015) 787–799.
[44] Saruchi, V. Kumar, Adsorption kinetics and isotherms for the removal of Rhodamine B dye and Pb^{+2} ions from aqueous solutions by a hybrid ion-exchanger, Arabian J. Chem., 12 (2019) 316–329.
[45] N. Ayawei, A.N. Ebelegi, D. Wankasi, Modelling and interpretation of adsorption isotherms, J. Chem., 2017 (2017) 1–11.
[46] K.Y. Foo, B.H. Hameed, Insights into the modeling of adsorption isotherm systems, Chem. Eng. J., 156 (2010) 2–10.
[47] H. Reza Ghaffari, H. Pasalari, A. Tajvar, K. Dindarloo, B.B. Goudarzi, V. Alipour, A. Ghanbarneajd, Linear and nonlinear two-parameter adsorption isotherm modeling: a case-study, Int. J. Eng. Sci., 6 (2017) 01–11.
[48] N.S. Yousef, R. Farouq, R. Hazzaa, Adsorption kinetics and isotherms for the removal of nickel ions from aqueous solutions by an ionexchange resin: application of two and three parameter isotherm models, Desal. Water Treat., 57 (2016) 21925–21934.
[49] A.A. Ahmad, B.H. Hameed, N. Aziz, Adsorption of direct dye on palm ash: kinetic and equilibrium modeling, J. Hazard. Mater., 141 (2007) 70–76.
[50] M.K. Dahri, M.R.R. Kooh, L.B.L. Lim, *Casuarina equisetifolia* cone as sustainable adsorbent for removal of Malachite green dye from aqueous solution using batch experiment method, Moroccan J. Chem., 6 (2018) 480–491.
[51] L.B.L. Lim, N. Priyantha, N.H. Mohd Mansor, Utilizing *Artocarpus altilis* (breadfruit) skin for the removal of malachite green: isotherm, kinetics, regeneration, and column studies, Desal. Water Treat., 57 (2015) 16601–16610.
[52] A. Moosavi, A.A. Amooey, A.A. mir, M.H. Marzbali, Extraordinary adsorption of acidic fuchsine and malachite green onto cheap nano-adsorbent derived from eggshell, Chin. J. Chem. Eng., 28 (2020) 1591–1602.
[53] N.A.H. Mohamad Zaidi, L. Biaw Leng Lim, A. Usman, M.R. Rahimi Kooh, Efficient adsorption of malachite green dye using *Artocarpus odoratissimus* leaves with artificial neural network modelling, Desal. Water Treat., 101 (2018) 313–324.
[54] R. Ahmad, R. Kumar, Adsorption studies of hazardous malachite green onto treated ginger waste, J. Environ. Manage., 91 (2010) 1032–1038.
[55] S.D. Khattri, M.K. Singh, Removal of malachite green from dye wastewater using neem sawdust by adsorption, J. Hazard. Mater., 167 (2009) 1089–1094.
[56] B.H. Hameed, M.I. El-Khaiary, Batch removal of malachite green from aqueous solutions by adsorption on oil palm trunk fibre: equilibrium isotherms and kinetic studies, J. Hazard. Mater., 154 (2008) 237–244.
[57] P. Saha, S. Chowdhury, S. Gupta, I. Kumar, Insight into adsorption equilibrium, kinetics and thermodynamics of Malachite Green onto clayey soil of Indian origin, Chem. Eng. J., 165 (2010) 874–882.
[58] A. Mittal, Adsorption kinetics of removal of a toxic dye, Malachite Green, from wastewater by using hen feathers, J. Hazard. Mater., 133 (2006) 196–202.
[59] B.H. Hameed, M.I. El-Khaiary, Malachite green adsorption by rattan sawdust: isotherm, kinetic and mechanism modeling, J. Hazard. Mater., 159 (2008) 574–579.
[60] L.B.L. Lim, N. Priyantha, K.J. Mek, N.A.H. Mohamad Zaidi, Application of *Momordica charantia* (bitter gourd) waste for the removal of malachite green dye from aqueous solution, Desal. Water Treat., 154 (2019) 385–394.
[61] E. Bulut, M. Özacar, İ. Ayhan Şengil, Adsorption of malachite green onto bentonite: equilibrium and kinetic studies and process design, Microporous Mesoporous Mater., 115 (2008) 234–246.